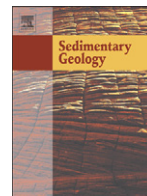




Contents lists available at ScienceDirect

## Sedimentary Geology

journal homepage: [www.elsevier.com/locate/sedgeo](http://www.elsevier.com/locate/sedgeo)

## Geochemistry of Cretaceous Oceanic Red Beds – A synthesis

Stephanie Neuhuber\*, Michael Wagreich

Universität Wien, Department für Geodynamik und Sedimentologie, Althanstrasse 14, 1090 Wien, Austria

## ARTICLE INFO

## Article history:

Received 25 July 2009

Received in revised form 20 October 2010

Accepted 21 October 2010

Available online xxx

## Keywords:

Upper Cretaceous

Marine red beds

Iron geochemistry

Geochemistry of marine red beds

## ABSTRACT

This paper summarizes the geochemistry of Cretaceous Oceanic Red Beds (CORBs), their depositional conditions and their significance in reconstructing marine environments. We report major and minor element compositions of carbonate, clayey, and siliceous CORBs and compare these with average element compositions of carbonates, deep sea carbonates, deep sea clays, and average shale compositions. Element distributions in carbonate CORBs are mostly similar to average carbonate compositions. In particular, Sr concentrations are more comparable to average carbonates than deep sea carbonate Sr concentrations. Clayey CORBs are high in Al, Ti, K, and Fe. Their minor element compositions are more similar to average shale than deep sea clay, which generally has higher values in minor elements. In comparison, siliceous CORBs have at least two times lower Al but higher Si concentrations than clayey CORBs. We further speculate on possible reactions involved in iron mobilization and CORB formation.

© 2010 Published by Elsevier B.V.

## 1. Introduction

The Late Cretaceous was a greenhouse period with considerable sea level changes and tectonic compression in the Tethyan belt that resulted in opening and closing of ocean basins (Stampfli et al., 2002; Wagreich and Faupl, 1994). A major characteristic of the Late Cretaceous global change was the evolution from anoxic to predominantly oxic conditions in the oceans which took place after the last global oceanic anoxic event OAE 2 (Hu et al., 2005).

This global climate change was a result of variations in the operating mode of various earth processes such as changes in palaeoceanography and palaeocirculation (e.g. Friedrich et al., 2008; Hay, 2008, 2009; Puceat et al., 2005), changes in palaeoproductivity (nutrient distribution, e.g. Neuhuber et al., 2007), tectonic processes (opening and closing of major seaways, migration of continental plates and subduction or expansion of ocean basins, e.g. Friedrich and Erbacher, 2006; Wagreich and Faupl, 1994), and climatic variations (change from greenhouse to icehouse conditions, e.g. Bice et al., 2006; Miller et al., 2005).

Periods of high primary production resulted in Oceanic Anoxic Events (OAEs) when vast amounts of organic material were buried in oceanic sediments (Larson, 1991; Pedersen and Calvert, 1990; Schlanger and Jenkyns, 1976). OAEs resulted in significant CO<sub>2</sub> fixation in marine sediments in the form of organic matter and can be correlated worldwide. In contrast to anoxic events, oceanic red beds were deposited under oxic conditions and are widespread and diachronous (Hu et al., 2005; Wagreich and Krenmayr, 2005) and

therefore reflect a state of the ocean system rather than a distinct and short stratigraphic level like OAEs.

The most significant worldwide change from anoxia to oxic deposition with the formation of CORBs (Cretaceous Oceanic Red Beds, Hu et al., 2005; Wang et al., 2009) deposition started after the global oceanic anoxic event OAE 2 in the early Turonian (Hu et al., 2006; Neuhuber et al., 2007; Wagreich et al., 2009). In the Santonian–Campanian a peak episode of worldwide enhanced CORB deposition is recognized globally (Wang et al., 2009, 2010–this volume). These changes in the deep sea recorded by pelagic sediments are more likely to reflect an overall climatic change as opposed to shallow seas where regional and seasonal influences may be more pronounced.

New ideas on oceanic circulation proposed by Hay (2008, 2009) for the Cretaceous differ fundamentally from modern ocean circulation. Thermohaline circulation drives the sea today whereas the Cretaceous sea – due to reduced deep water formation at largely ice free poles – was probably characterized by slow vertical water exchange. The vertical and latitudinal temperature gradient was smaller compared to the modern ocean and resulted in large regional eddies (Hay, 2008).

This paper investigates the geochemistry of CORBs in detail. Based on a review of published data (Bak, 2007; Baltuck, 1982; Hikoroa et al., 2009; Jiang et al., 2009; Neuhuber and Wagreich, 2009; Neuhuber et al., 2007) we classify CORBs according to their chemical composition.

## 2. Material, methods and data

Cretaceous Oceanic Red Beds cover a wide range of lithologies that range from shallow water deposits (Wiese, 2009) to deposits below CCD (Wagreich et al., 2009). The sedimentology of these deposits was

\* Corresponding author. Fax: +43 1 4277 9534.

E-mail addresses: [stephanie.neuhuber@univie.ac.at](mailto:stephanie.neuhuber@univie.ac.at) (S. Neuhuber), [michael.wagreich@univie.ac.at](mailto:michael.wagreich@univie.ac.at) (M. Wagreich).

elucidated by Hu et al. (2005, 2006), Wagreich and Krenmayr (2005) and Wagreich et al. (2009), among others. Geochemical studies dealing with element distribution in CORBs include studies from Italy (Calderoni and Ferrini, 1984; Hu et al., 2009), from the Alps (Neuhuber et al. 2007; Neuhuber and Wagreich, 2009; and XRF data presented in this paper), New Zealand (Hikoroa et al., 2009), the Polish Flysch Carpathians (Bak, 2007; Jiang et al., 2009) and siliceous sediments from the Pindos Zone (Baltuck, 1982).

This paper compiles X-ray fluorescence spectrometry (XRF) data from the literature (authors previously mentioned) in different palaeogeographic settings as well as some data points from an Austroalpine Profile (Brandenberg, Austria). Table 1 gives an overview of the number of samples in each profile and their main element composition. Minor element distributions are given in Tables 2 and 3. Austrian and Italian CORBs contain significant amounts of calcium carbonate ranging between 50% and 98%. Samples from New Zealand (Manganotone section, Hikoroa et al., 2009), from the Polish Flysch (Trzemesnia section, Bak, 2007 and Mazak section, Jiang et al., 2009) are free of biogenic carbonate.

### 2.1. Lithology and age constraints of discussed profiles

Four profiles are set in the Tethys ocean: Vispi (Italy), Rehkogelgraben (Austria, Ultrahelvetics), Buchberg (Austria, Ultrahelvetics) and Brandenberg (Austria, Austroalpine). The Vispi section (Fig. 1) contains Scaglia Rossa limestones of Turonian age. Sediments from Buchberg and Rehkogel (Ultrahelvetics) are red marl – limestone cycles of Turonian (Buchberg) and Santonian (Rehkogelgraben) age. Brandenberg was situated at the active margin of the Austroalpine microplate (Fig. 1). Both sections at Karpenision and Plaka from the Pindos ocean cover red marlstones of Santonian age. The Manganotone section consists of Turonian mudstone deposited on a passive continental margin. The variegated shales from the Polish Flysch

Carpathians in Trzemesnia are of early Turonian age and those of the Mazak section of Cenomanian age.

### 2.2. Data presentation

Wagreich et al. (2009) and Wang et al. (2009) introduced a classification of CORBs with three end members: siliceous CORBs, carbonate CORBs, and clayey CORBs (Fig. 2A). This scheme is based on the classification of recent pelagic-hemipelagic sediments as calcareous ooze, siliceous ooze, and red pelagic clays (Hay et al., 1984). We plot geochemical data in a similar fashion with the end members Ca (for carbonate production) assuming negligible amounts of feldspar, Si, and Al. This representation is not directly comparable to the classification of CORBs introduced by Wagreich et al. (2009), because it characterizes CORBs according to their chemical composition.

## 3. Compilation and discussion of geochemical data

### 3.1. CORB geochemistry worldwide

The comparison of bulk XRF was fit to the three end members: calcium, silica, and aluminium. Al concentrations never reach the average shale value (Turekian and Wedepohl, 1961) of 50% but range around 25%. The average composition of deep sea carbonates (Turekian and Wedepohl, 1961, DC, Fig. 2) lies below the values of the Vispi Quarry (Hu et al., 2009). Average values from Manganotone (New Zealand) and from the Pindos Zone (Greece) plot a little above 75% Si but samples from the Pindos are higher in Ca (Fig. 2). Three sections are virtually free of Ca: Manganotone (New Zealand), Trzemesnia (Polish Flysch) and the Mazak section (Flysch, Czech Republic). Deposition below CCD of these siliceous clays and the distal deposition without any Ca-bearing minerals such as plagioclase is the reason for this depletion. These three sections plot in the vicinity of

**Table 1**  
Bulk composition: average main element distribution in CORBs.

Section	Author(s)	n	Al		Ca		Si	
			Avg	Stdev	Avg	Stdev	Avg	Stdev
Manganotone	Hikoroa et al., 2009	7	119.3	6.6	9.3	7.7	304.0	4.3
Trzemesnia	Bak, 2007	13	90.8	7.1	5.3	0.5	305.3	7.8
Mazak	Jiang et al., 2009	16	101.5	7.3	3.6	1.4	315.9	7.2
Karpenision	Baltuck, 1982	2	46.2	16.2	77.0	96.5	248.2	36.1
Plaka	Baltuck, 1982	4	4.8	3.2	89.3	167.8	343.7	180.2
Vispi	Hu et al., 2009	20	0.3	0.1	379.4	8.3	16.2	6.2
Rehkogel	Neuhuber and Wagreich, 2009	4	45.8	4.6	234.8	18.2	122.7	12.9
Buchberg	Neuhuber et al., 2007	7	46.2	10.3	225.3	30.4	133.9	22.3
Brandenberg	this work	4	55.1	6.0	192.9	22.6	124.8	9.6
Avg shale	Turekian and Wedepohl, 1961		80		22.1		73	
Avg carbonate			4.2		302.3		24	
Deep sea carbonate			20		312.4		32	
Deep sea clay			84		29		250	

Section	n	Fe		K		Mg		Mn		Na		P		Ti	
		Avg	Stdev	Avg	Stdev	Avg	Stdev	Avg	Stdev	Avg	Stdev	Avg	Stdev	Avg	Stdev
Manganotone	7	66.9	10.9	53.1	5.2	12.4	0.4	0.5	74.3	26.3	1.0	1.0	0.1	4.1	0.5
Trzemesnia	13	47.0	13.8	37.4	4.0	9.8	0.6	0.3	0.3	3.5	0.4	0.4	0.1	3.2	0.3
Mazak	16														
Karpenision	2	53.6	33.4					1.7	0.1					2.9	1.7
Plaka	4	3.7	2.0					0.6	0.6					1.4	2.2
Vispi	20	1.8	1.0	1.9	0.5	2.3	0.2	0.5	0.1	0.3	0.1	0.2	0.1	0.1	0.0
Rehkogel	4	22.0	2.9	12.2	1.7	7.0	0.8	0.4	0.0	1.7	0.4	0.3	0.0	1.9	0.2
Buchberg	7	19.5	6.9	10.9	3.4	7.7	1.2	0.3	0.1	1.9	1.1	0.5	0.2	2.0	0.5
Brandenberg	4	35.8	4.5	30.8	2.1	28.2	7.8	0.7		3.5	1.2	0.3	0.1	1.8	0.3
Avg shale		47.2		26.6		15		0.85		9.6		0.7		4.6	
Avg carbonate		3.8		2.7		47		1.1		0.4		0.4		0.4	
Deep sea carbonate		9		2.9		4		1		20		0.35		0.77	
Deep sea clay		65		25		21		6.7		40		1.5		4.6	

n = number of samples.

All data are XRF data in mg/g.

**Table 2**

Bulk composition: average minor element distribution in CORBs.

Section	n	Ba		Co		Cr		Cu		Ni		Pb		
		Avg	Stdev	Avg	Stdev	Avg	Stdev	Avg	Stdev	Avg	Stdev	Avg	Stdev	
Manganotone	Clayey CORB	7	0.19	0.17			75.02	12.00	53.75	10.12	40.07	4.08		
Trzeesnia		13	248.08	78.21	24.00	22.56	76.31	17.00	131.08	163.61	67.46	20.42	45.15	46.60
Mazak		16	362.31	40.13	21.27	1.46	68.94	6.05	68.08	41.42	51.50	3.19	23.00	7.81
Vispi	Carbonate CORB	20	294.96	323.62	1.67	1.00	7.77	2.42	9.89	6.99	4.25	3.08	3.27	1.50
Rehkogel		4	306.13	213.37	5.93	0.62	50.54	9.08	18.06	1.61	34.57	4.56	11.94	0.27
Buchberg		7	756.41	1622.33	5.97	0.90	53.85	23.39	87.07	62.48	31.55	8.51	10.53	1.82
Brandenberg		4	165.07	61.87	6.49	5.14	62.98	82.20	10.59	7.97	58.98	46.61	10.03	4.01
Gubbio		29							13.10	7.4			6.10	3
Avg shale	Al end member		580		19.00		90.00		45.00		68.00		20.00	
Avg carbonate	Ca end member		10		0.10		11.00		4.00		20.00		9.00	
Deep sea carbonate			190		7.00		11.00		30.00		30.00		9.00	
Deep sea clay	Si end member		2300		74		90		250.00		225.00		80.00	

Section	n	Rb		Sr		U		V		Zn		Zr		
		Avg	Stdev	Avg	Stdev	Avg	Stdev	Avg	Stdev	Avg	Stdev	Avg	Stdev	
Manganotone	Clayey CORB	7	193.71	28.69	166.51	40.41					102.38	8.88	159.40	14.00
Trzeesnia		13	112.31	19.22	114.69	10.20	3.61	1.51			80.92	17.70		
Mazak		16	130.81	18.14	77.41	13.35	1.58	0.57	112.06	26.77	84.74	32.83	94.73	20.49
Vispi	Carbonate CORB	20	67.06	10.74	449.72	21.76	2.67	0.40	61.31	9.80	52.31	4.80	43.53	5.16
Rehkogel		4			492.34	71.10	0.10	0.04	5.46	2.71	17.24	8.62	3.00	1.57
Buchberg		7	54.33	17.01	376.78	35.42	2.70	0.32	91.44	106.91	54.84	13.40	38.65	10.74
Brandenberg		4	35.31	43.94	414.83	149.11	0.43	0.18	33.98	38.84	29.24	27.32	70.33	5.76
Gubbio		29									24.93	15.1		
Avg shale	Al end member		140.00		300.00		3.70		130.00		95.00		160.00	
Avg carbonate	Ca end member		3.00		610.00		2.20		20.00		20.00		19.00	
Deep sea carbonate			10.00		2000.00				20.00		35.00		20.00	
Deep sea clay	Si end member		11.00		180.00		1.30		120.00		165.00		150.00	

n = number of samples.

All data in this table are XRF data in µg/g.

No data from Karpenision and Plaka.

average deep sea clay (DSC in Fig. 2, Turekian and Wedepohl, 1961). Levels at or close to average shale composition (i.e. the Al end member, Fig. 2: AS) are never reached in all CORBs listed in Table 1. Average shale values originate from an environment with high detrital influx and were deposited in a proximal or shallow water setting (Wedepohl, 1968). Our results correspond well with the distal nature of CORBs even though Table 1 might not cover all their varieties. All samples but those from the Vispi quarry are mixtures between the Al end member and the Si end member.

Bulk geochemical data of Al vs. K, Ti, and Fe including average values for shale, carbonate, deep sea carbonate and deep sea clay as reference points correlate positively (Fig. 3). All those elements are of terrigenous origin and indicate that the chemical composition of most samples is a function of the primary sediment composition. Major diagenetic remobilization is not indicated in these diagrams.

### 3.2. Calcium end member: Ultrahelvetic and Vispi section

Carbonate CORBs tend to have a composition similar to average carbonate values of Turekian and Wedepohl (1961). In comparison, average deep sea carbonate is generally higher in minor elements, in particular in Sr with on average 2000 ppm in deep sea carbonates as opposed to 500 ppm for average carbonates and carbonate CORBs. This most likely reflects the carbonate production in the surface water.

Ultrahelvetic sediments contain a high portion of carbonate (at least above 50%) in the form of calcite formed mostly by calcareous nannoplankton and (mainly planktic) foraminifera (Neuhuber et al., 2007; Wagreich et al., 2009). The terrigenous fraction such as phyllosilicates, quartz, and plagioclase is very fine-grained and consists largely of sheet silicates. Organic carbon preservation is very low in this environment and sediment accumulation rates are

**Table 3**

Carbonate associated main elements; below: minor and trace elements.

Section	Author(s)	n	Al		Ca		Si	
			Avg	Stdev	Avg	Stdev	Avg	Stdev
Vispi	Hu et al., 2009				379.43	8.2807	16.203	6.1753
Rehkogel	Neuhuber and Wagreich, 2009	70	0.336	0.2708	246.94	48.2		
Buchberg	Neuhuber et al., 2007	57	0.389	0.2439	370.64	28.661		
Brandenberg	this work	4	0.6231	0.0593	322.04	30.23		
Oberhehenfeld	submitted	35	50.15	44.878	24.285	2.8175		

Section	n	Fe		K		Mg		Mn		P		Ti	
		Avg	Stdev	Avg	Stdev	Avg	Stdev	Avg	Stdev	Avg	Stdev	Avg	Stdev
Rehkogel	70	1.4	0.3			0.8	0.2	0.3	0.1	0.1	0.0		0.0
Buchberg	57	0.4	0.2			1.6	0.4	0.4	0.1	0.2	0.7	0.3	0.1
Brandenberg	4	4.1	0.8	1.1	0.1	47.0	21.7	0.9	0.1	0.2	0.0		
Oberhehenfeld	35	1.8	0.8	1.2	0.6	1.4	0.2	1.2	0.3			706.8	0.1

n = number of samples.

All data in this table are carbonate associated elements in mg/g.

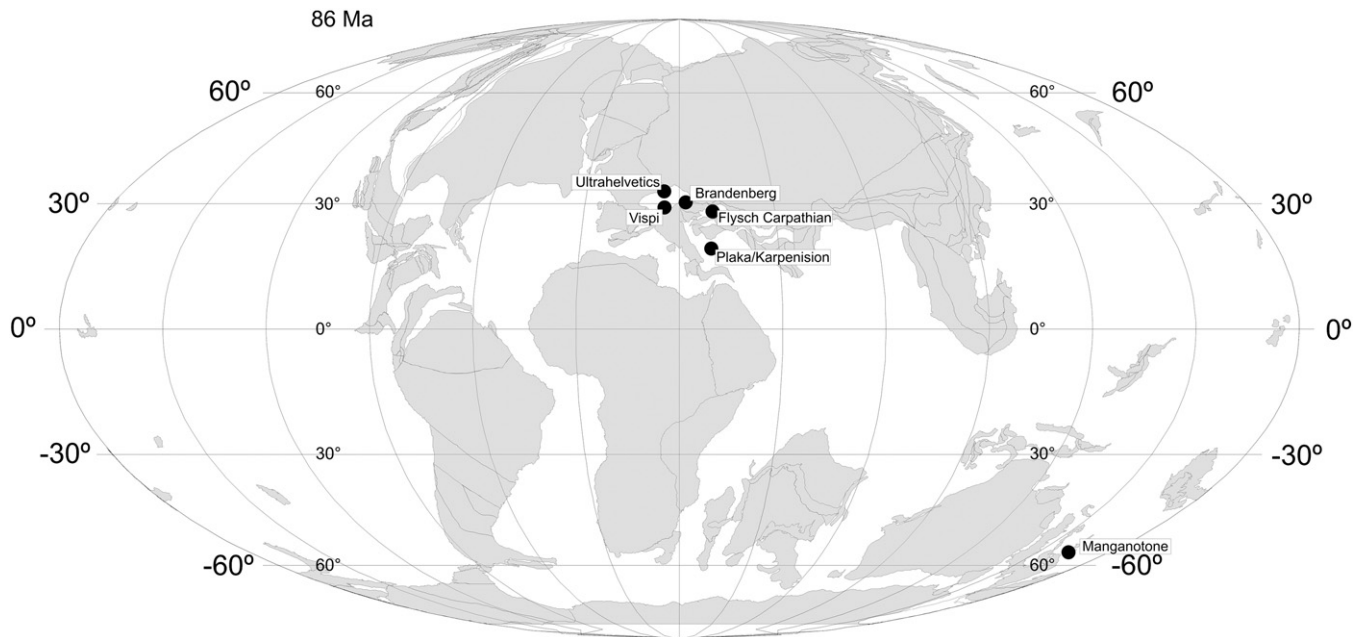


Fig. 1. Paleogeographic map (Schettino and Scotese, 2002) indicating positions of discussed profiles.

typically below 10 mm/kyr (Neuhuber and Wagreich, 2009; Neuhuber et al., 2007) as in today's deep sea clays (1–10 mm/kyr) or coccolith oozes (10–50 mm/kyr, Tucker and Wright, 1990). As to the relative Al, Si, and Ca content Fig. 2 places samples from the Buchberg, Rehkogel, and Brandenburg sections (Northern Calcareous Alps, see Wagreich et al., 2009) in between the mixing lines of Ca dominated CORBs and Al and Si CORBs.

### 3.3. Silica end member: Pindos Zone

Fig. 3 shows an overall positive correlation of Si and Al but higher Si concentrations in the Pindos samples. Al and Ti (Fig. 3) correlate positively where the Pindos samples lie within the general trend. This is most likely caused by a large contribution of biogenic silica to the

Pindos samples (Karpenision = BK and Plaka = BP) samples that results in a relative enrichment of Si compared to Ti. Al and Ca correlate negatively (Fig. 3), but samples from BR and BK from the Pindos Zone lie below the mixing line due to the setting below CCD. Unfortunately no minor elements are reported from the Karpenision and Plaka sections.

### 3.4. Aluminium end member: samples from the Carpathians and New Zealand

In general, the Al-rich end member has similar to average shale (Table 2) whereas deep sea clay element concentration tends to be generally higher. Of all samples those from New Zealand have highest contents in Ti, Al, Si, Fe, K, Na, Rb (Figs. 3 and 4). The Carpathian

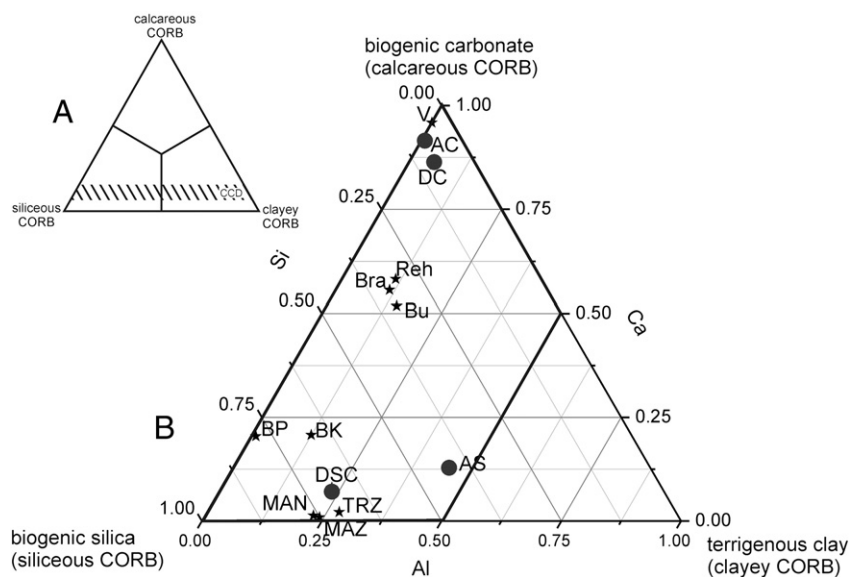
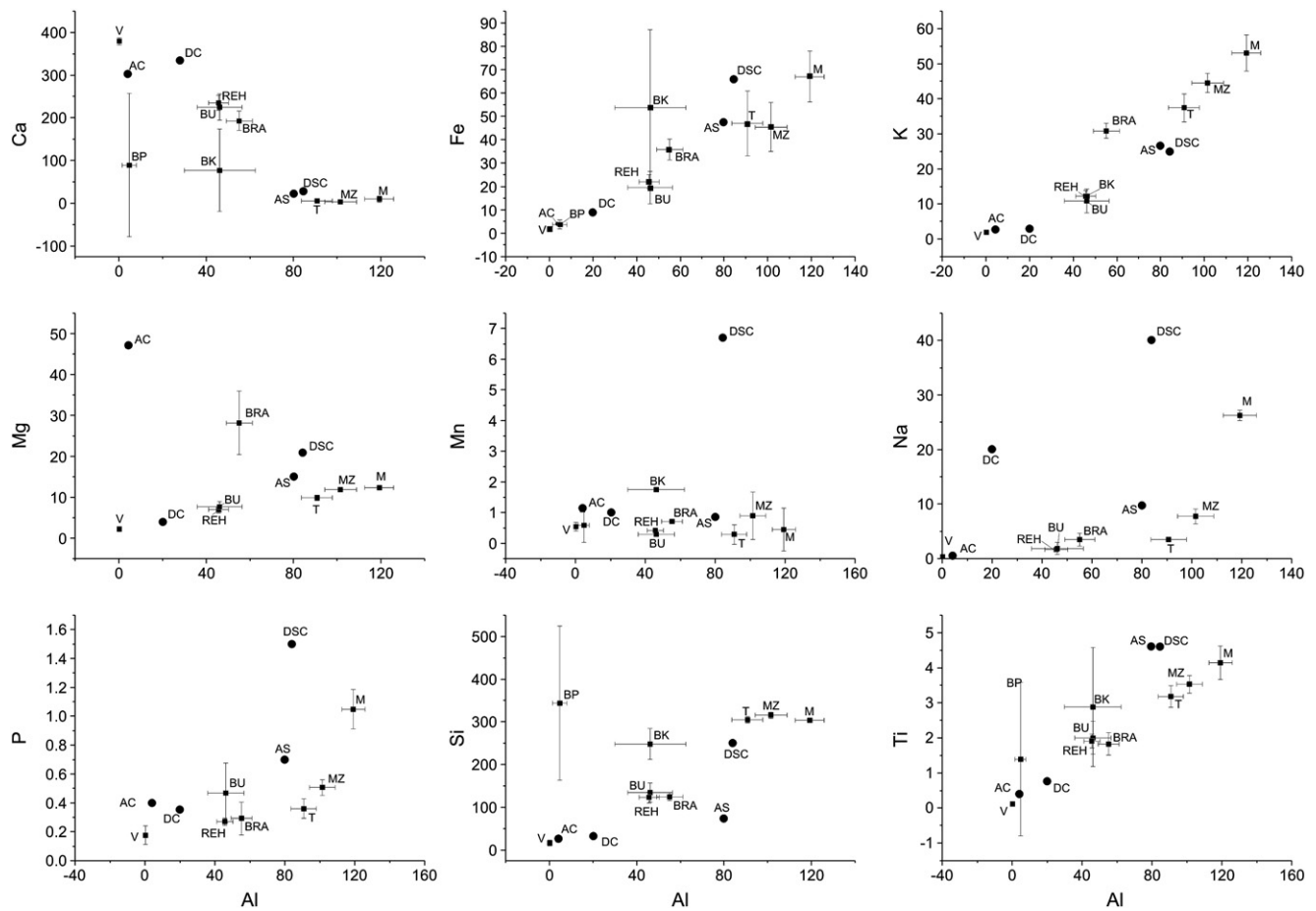


Fig. 2. A. Classification of CORBs (Wagreich et al., 2009); B. Triangle classification of bulk geochemical data with Al, Si, and Ca end members; big black dots represent average values from Turekian and Wedepohl, 1961 for average carbonate (AC) deep sea carbonate (DC), deep sea clay (DSC), average shale (AS); Austria (Ultrahelvetics): Bra = Brandenburg, Reh = Rehkogelgraben, Bu = Buchberg; Greece (Peloponnes): BP = Plaka, BK = Karpenision; New Zealand: MAN = Manganotone; Flysch Carpathians: TRZ = Trzemesnia, MAZ = Mazak; Italy (Scaglia): V = Vispi.



**Fig. 3.** (XRF) Main elements vs. Al; average values from [Turekian and Wedepohl, 1961](#): AC = average carbonate; DC = deep sea carbonate, DSC = deep sea clay, AS = average shale; Austria (Ultrahelvetics): BRA = Brandenburg, REH = Rehkogelgraben, BU = Buchberg; Greece (Peloponnes): BP = Plaka, BK = Karpeneion; New Zealand: MAN = Manganotone; Flysch Carpathians: TRZ = Trzemesnia, MAZ = Mazak; Italy (Scaglia): V = Vispi.

sections may be separated by minor element distribution from the Manganotone, NZ samples ([Table 2, Fig. 4](#)). This suggests a primary sediment source high in alkaline metals such as intrusive rocks rich in feldspar. Concerning minor elements, Trzemesnia is higher in Cu, Co, Ni, Pb and U which is most likely caused by the occurrence of ferromanganese nodules ([Bak, 2006, 2007](#)) in some parts of the profile.

### 3.5. Color origin of CORBs

Throughout earth's history the occurrence of red colored strata is commonly attributed to increased iron oxide content. Increased bulk iron concentration in red foraminifer tests (max 14 mg/g in red tests and max 3.5 mg/g in white tests) demonstrates that iron oxides cause the red colours of our studied CORBs as well. In contrast, carbonate associated iron is higher in white samples compared to red samples ([Neuhuber and Wagreich, 2009](#)). Occasionally, both red and white varieties of foraminifer tests occur within one bed in the Ultrahelvetic Realm.

The primary source of iron is terrigenous material. In all available bulk geochemical data from XRF measurements or HF-HNO<sub>3</sub> digestion Al and Fe correlate positively (Buchberg:  $R=0.96$ ; Rehkogelgraben:  $R=0.99$ ; Schmidssippl:  $R=0.87$ ; and Brandenburg:  $R=0.97$ ) and indicate a detrital iron source. [Neuhuber et al. \(2007\)](#) found smectite, chlorite and illite clays in the detrital fraction that may serve as source of iron. Iron concentrations are highest and most variable in siliceous CORBs ([Table 1](#)) caused by relatively higher terrigenous influence.

Low values – below average carbonate concentration – are reported from relatively pure carbonate rocks of Vispi Quarry ([Hu et al., 2009](#)).

Because of fast oxidation rates ([Millero et al., 1987](#)) of ferrous iron, Fe may be used as indicator for the oxygenation state of an environment. During oxic conditions ferric iron ( $Fe^{3+}$ ) is stable as iron (hydr)oxide and during anoxic conditions ferrous iron ( $Fe^{2+}$ ) forms sulfides. After the bacterially mediated transition of oxidized to reduced iron,  $Fe^{2+}$  ions may diffuse freely in the pore space and react with other mineral surfaces such as clays, or carbonates.

### 3.6. Speculation on iron mobilization and biogeochemical aspects

Possible reactions resulting in CORB formation are dissolution of terrigenous iron oxides or iron bearing clays by microbial  $Fe^{3+}$  reduction as hypothesized by [Mamet and Preat \(1996\)](#) followed by adsorption of mobile ferrous iron onto calcite cleavages. The local depletion in oxygen that is necessary for Fe to diffuse might be a result of decreased bottom water oxygenation or increased sediment accumulation rates where fine-grained flaky particles cover pore space.

Reduction most likely does not occur as sediment-surface-parallel redox front but in discrete zones with a lower Eh due to small-scale inhomogeneities in initial TOC content.

In carbonate free settings reduced iron will not be incorporated into calcite but will be oxidized to iron oxides. In these settings iron may there be accumulated during organic matter degradation but is completely reoxidized.

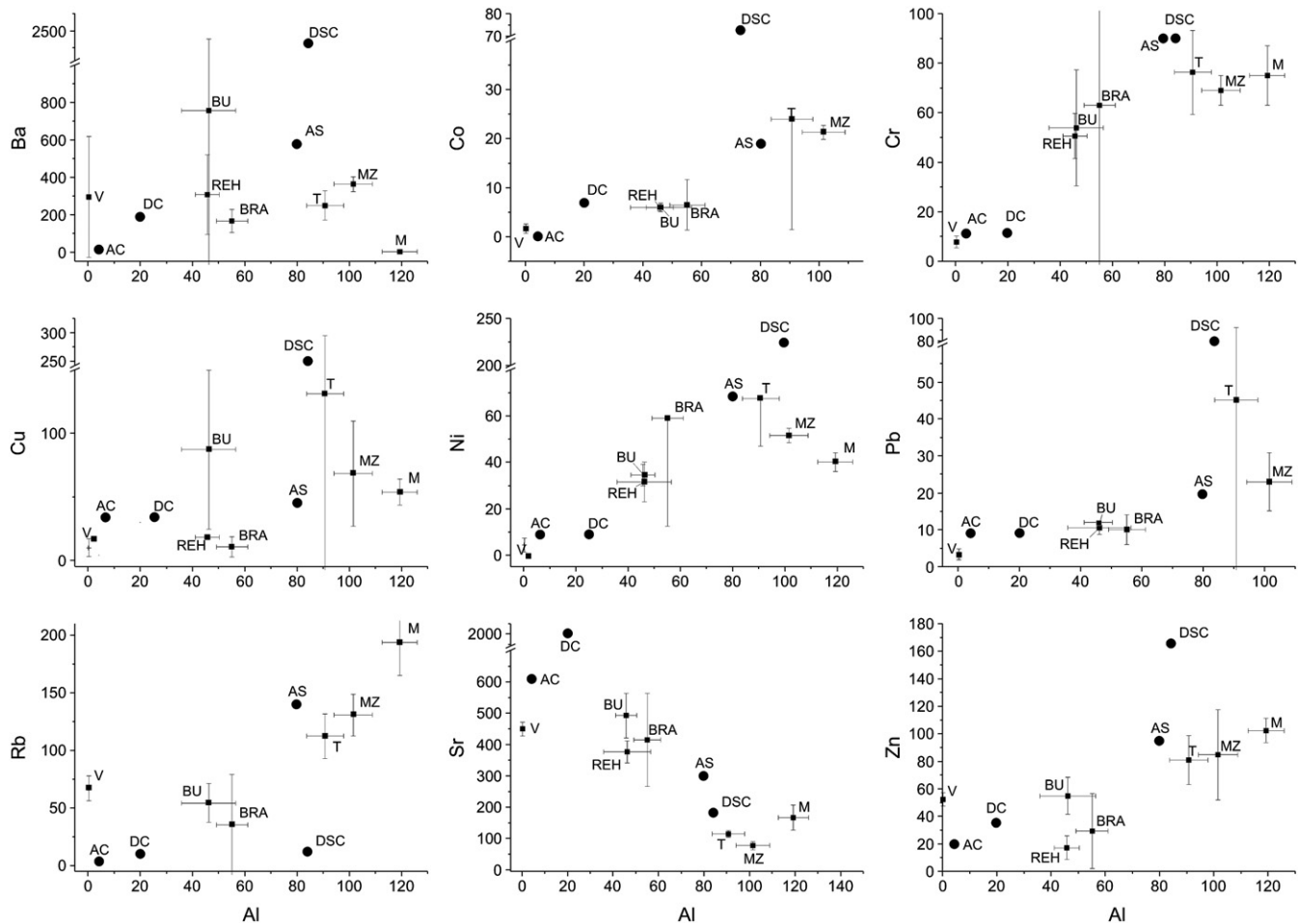


**Fig. 4.** (XRF) Minor elements vs. Al; average values from Turekian and Wedepohl, 1961: AC = average carbonate; DC = deep sea carbonate, DSC = deep sea clay, AS = average shale; Austria (Ultrahelvetics): BRA = Brandenberg, REH = Rehkogelgraben, BU = Buchberg; Greece (Peloponnes): BP = Plaka, BK = Karpeneion; New Zealand: MAN = Manganotone; Flysch Carpathians: TRZ = Trzemesnia, MAZ = Mazak; Italy (Scaglia): V = Vispi.

#### 4. Conclusion

We use bulk geochemical data to characterize CORBs according to their element distribution within Ca, Al, and Si, end members.

Carbonate CORBs are high in Ca and carbonate associated elements (mainly Sr) and they are comparable to average carbonate as opposed to deep sea carbonate. This is most likely caused by biogenic carbonate export from the surface water.

Clayey CORBs are highest in terrigenous elements. However, the element distribution in clayey CORBs from New Zealand and the Carpathians differ concerning their trace element distribution where New Zealand has high alkali metal concentrations. One Carpathian section is influenced by ferromanganese nodule precipitation that results in higher in Co, Cu, Ni, and Pb concentrations.

Siliceous CORBs are identified in their Al, Si, and Ti distribution where Al and Ti correlate positively and Si is on average higher compared to clayey or carbonate CORBs.

Iron oxides cause the red color in CORBs. The main fraction of iron in CORB sediments is fixed in silicate lattices and immobile. During early diagenetic reactions some of the iron (esp. in sheet silicates) may be mobilized by microbial action.

#### Acknowledgements

This research was funded by a doctoral grant of the Austrian Academy of Sciences and a scholarship of the University of Vienna. We thank Stephan Krämer (Vienna) for review and discussion on the

geochemistry section. Wilfried Körner and Andi Doll are acknowledged for help with the ICP-MS analyses. The reviewers of this article are acknowledged. Field work was supported by IGCP 463 and IGCP 555 grants.

#### References

- Bak, K., 2006. Sedimentological, geochemical and microfossil responses to environmental changes around the Cenomanian–Turonian boundary in the Outer Carpathian Basin; a record from the Subsilurian Nappe, Poland. *Palaeogeography, Palaeoclimatology, Palaeoecology* 237, 335–358.
- Bak, K., 2007. Deep-water facies succession around the Cenomanian–Turonian boundary in the Outer Carpathian basin: sedimentary, biotic and chemical records in the Silesian Nappe, Poland. *Palaeogeography, Palaeoclimatology, Palaeoecology* 248, 255–290.
- Baltuck, M., 1982. Provenance and distribution of Tethyan pelagic and hemipelagic siliceous sediments, Pindos Mountains, Greece. *Sedimentary Geology* 31, 63–88.
- Bice, K.L., Birgel, D., Meyers, P.A., Dahl, K.A., Hinrichs, K.-U., Norris, R.D., 2006. A multiple proxy and model study of Cretaceous upper ocean temperatures and atmospheric CO<sub>2</sub> concentrations. *Paleoceanography* 21, PA2002. doi:10.1029/2005PA001203.
- Calderoni, G., Ferrini, V., 1984. Abundances and chemical fractionation of Al, Fe, Mn, Zn, Pb, Cu and Ti in Cretaceous–Palaeocene limestones from Gubbio (Central Italy). *Geochemical Journal* 18, 31–41.
- Friedrich, O., Ehrbacher, J., 2006. Benthic foraminiferal assemblages from Demerara Rise (ODP Leg 207, western tropical Atlantic): possible evidence for a progressive opening of the Equatorial Atlantic Gateway. *Cretaceous Research* 27, 377–397.
- Friedrich, O., Erbacher, J., Moriya, K., Wilson, P.A., Kuhnert, H., 2008. Warm saline intermediate waters in the Cretaceous tropical Atlantic Ocean. *Nature Geoscience* 1, 453–457.
- Hay, W., 2008. Evolving ideas about the Cretaceous climate and ocean. *Cretaceous Research* 29, 725–753.
- Hay, W.W., 2009. Cretaceous oceans and ocean modeling. In: Hu, X.M., Wang, C.S., Scott, R.W., Wagreich, M., Jansa, L. (Eds.), *Cretaceous Oceanic Red Beds: Stratigraphy,*

- Composition, Origins, Paleoceanographic, and Paleoclimatic Significance: SEPM Special Publication, 91, pp. 243–271. Tulsa, OK.
- Hay, W.W., Sibuet, J.C., et al., 1984. Initial reports of the deep sea drilling project. 75, 1303 pp. US Government Printing Office, Washington DC.
- Hikoroo, D.C.H., Crampton, J., Field, B., Schiøler, P., 2009. Upper Cretaceous oceanic red beds in New Zealand. In: Hu, X.M., Wang, C.S., Scott, R.W., Wagreich, M., Jansa, L. (Eds.), *Cretaceous Oceanic Red Beds: Stratigraphy, Composition, Origins, Paleoceanographic, and Paleoclimatic Significance: SEPM Special Publication, 91*, pp. 137–145. Tulsa, OK.
- Hu, X.M., Jansa, L., Wang, C.S., Sarti, M., Bak, K., Wagreich, M., Michalik, J., Sotak, J., 2005. Upper Cretaceous oceanic red beds (CORBs) in the Tethys: occurrences, lithofacies, age, and environments. *Cretaceous Research* 26, 3–20.
- Hu, X., Jansa, L., Sarti, M., 2006. Mid-Cretaceous oceanic red beds in the Umbria–Marche basin, central Italy: constraints on paleoceanography and paleoclimate. *Palaeogeography, Palaeoclimatology, Palaeoecology* 233, 163–186.
- Hu, X., Cheng, W., Ji, J., 2009. Origin of Cretaceous Oceanic Red Beds from the Vispi Quarry Section, Central Italy: Visible Reflectance and Inorganic Geochemistry. In: Hu, X., Wang, C., Scott, R.W., Wagreich, M., Jansa, L. (Eds.), *Cretaceous Oceanic Red Beds: Stratigraphy, Composition, Origins, Paleoceanographic, and Paleoclimatic Significance: SEPM Special Publication, 91*, pp. 183–197. Tulsa, OK.
- Jiang, S.Y., Jansa, L., Skupien, P., Yang, J.H., Vasicek, Z., Hu, X., Zao, K.D., 2009. Geochemistry of intercalated red and gray pelagic shales from the Mazak formation of Cenomanian age in Czech Republic. *Episodes* 32, 3–12.
- Larson, R.L., 1991. Latest pulse of Earth: evidence for a mid-Cretaceous superplume. *Geology* 19, 457–550.
- Mamet, B., Preat, A., 1996. Iron-bacterial mediation in Phanerozoic red limestones: state of the art. *Sedimentary Geology* 186, 147–157.
- Miller, K.G., Wright, J.D., Browning, J.V., 2005. Visions of ice sheets in a greenhouse world. *Marine Geology* 217, 215–231.
- Millero, F.J., Sotolongo, S., Izaguirre, M., 1987. The oxidation-kinetics of Fe(II) in seawater. *Geochimica et Cosmochimica Acta* 51, 793–801.
- Neuhuber, S., Wagreich, M., 2009. Geochemical characterization of Santonian cyclic oceanic red beds in the Alpine Tethys (Rehkogelgraben section, Austria). In: Hu, X.M., Wang, C.S., Scott, R.W., Wagreich, M., Jansa, L. (Eds.), *Cretaceous Oceanic Red Beds: Stratigraphy, Composition, Origins, Paleoceanographic, and Paleoclimatic Significance: SEPM Special Publication, 91*, pp. 199–207. Tulsa, OK.
- Neuhuber, S., Wagreich, M., Wendler, I., Spötl, C., 2007. Turonian oceanic red beds in the Eastern Alps: concepts for paleoceanographic changes in the Mediterranean Tethys. *Palaeogeography, Palaeoclimatology, Palaeoecology* 251, 222–238.
- Pedersen, T.F., Calvert, S.E., 1990. Anoxia versus productivity: what controls the formation of organic carbon rich sediments and sedimentary rocks? *American Association of Petroleum Geologists Bulletin* 74, 454–466.
- Puceat, E., Lecuyer, C., Reisberg, L., 2005. Neodymium isotope evolution of NW Tethyan upper ocean waters throughout the Cretaceous. *Earth and Planetary Science Letters* 236, 705–720.
- Schettino, A., Scotese, C., 2002. Global kinematic constraints to the tectonic history of the Mediterranean region and surrounding areas during the Jurassic and Cretaceous. *Journal of the Virtual Explorer* 8, 149–168.
- Schlanger, S.O., Jenkyns, H., 1976. Cretaceous oceanic anoxic events: causes and consequences. *Geologie en Mijnbouw* 55, 179–184.
- Stampfli, G.M., Borel, G., Marchant, R., Mosar, J., 2002. Western Alps geological constraints on western Tethyan reconstructions. *Journal of the Virtual Explorer* 8, 77–106.
- Tucker, M.E., Wright, V.P., 1990. *Carbonate Sedimentology*. Blackwell, p. 421.
- Turekian, K.K., Wedepohl, K.H., 1961. Distribution of the elements in some major units of the earth's crust. *Geological Society of America Bulletin* 72 (2), 175–191.
- Wagreich, M., Faupl, P., 1994. Palaeogeography and geodynamic evolution of the Gosau group of the Northern Calcareous Alps (Late Cretaceous, Eastern Alps, Austria). *Palaeogeography, Palaeoclimatology, Palaeoecology* 110, 235–254.
- Wagreich, M., Krenmayr, H.G., 2005. Upper Cretaceous oceanic red beds (CORB) in the Northern Calcareous Alps (Nierental Formation, Austria): slope topography and clastic input as primary controlling factors. *Cretaceous Research* 26, 57–64.
- Wagreich, M., Neuhuber, S., Egger, J., Wendler, I., Scott, R.W., Malata, E., Sanders, D., 2009. Cretaceous oceanic red beds (CORBs) in the Austrian Eastern Alps: passive-margin vs. active-margin depositional settings. In: Hu, X.M., Wang, C.S., Scott, R.W., Wagreich, M., Jansa, L. (Eds.), *SEPM Special Publication, 91*, pp. 37–91. Tulsa, OK.
- Wang, C.S., Hu, X., Huang, Y., Scott, R.W., Wagreich, M., 2009. Overview of Cretaceous Oceanic Red Beds (CORBs): a window on global oceanic/climate change. In: Hu, X.M., Wang, C.S., Scott, R.W., Wagreich, M., Jansa, L. (Eds.), *Cretaceous Oceanic Red Beds: Stratigraphy, Composition, Origins, Paleoceanographic, and Paleoclimatic Significance: SEPM Special Publication, 91*, pp. 13–35. Tulsa, OK.
- Wang, C., Hu, X., Huang, Y., Wagreich, M., Scott, R., Hay, W., 2010-this volume. Cretaceous oceanic red beds as possible consequence of oceanic anoxic events. *Sedimentary Geology*. doi:10.1016/j.sedgeo.2010.06.025.
- Wedepohl, K.H., 1968. Chemical fractionation in the sedimentary environment. In: Ahrens, L.H. (Ed.), *Origin and Distribution of the Elements*. Pergamon Press, England, pp. 999–1016.
- Wiese, F., 2009. The Söhlde Formation (Cenomanian, Turonian, upper Cretaceous) NW Germany: shallow marine Pelagic red beds. In: Hu, X.M., Wang, C.S., Scott, R.W., Wagreich, M., Jansa, L. (Eds.), *Cretaceous Oceanic Red Beds: Stratigraphy, Composition, Origins, Paleoceanographic, and Paleoclimatic Significance: SEPM Special Publication, 91*, pp. 153–171. Tulsa, OK.